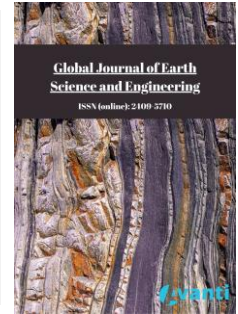




Published by Avanti Publishers
**Global Journal of Earth Science
and Engineering**

ISSN (online): 2409-5710




Comparing and Evaluating Ensemble Generation Techniques from Multi-Model Climate Data for Wind Speed Projection in Rio Grande do Norte for the Present and Future

Augusto de R.C. Gurgel * and Roberta T.S.F.D. Alves 

Federal Institute of Education, Science and Technology of Rio Grande do Norte (IFRN), Brazil

ARTICLE INFO

Article Type: Research Article

Academic Editor: Zhenkun Tian 

Keywords:

RCP8.5

CORDEX

Wind energy

Arithmetic mean

Convex combination

Regional climate models

Timeline:

Received: February 15, 2025

Accepted: May 15, 2025

Published: June 25, 2025

Citation: Gurgel ARC, Alves RTSFD. Comparing and evaluating ensemble generation techniques from multi-model climate data for wind speed projection in Rio Grande do Norte for the present and future. Glob J Earth Sci Eng. 2025; 12: 14-29.

DOI: <https://doi.org/10.15377/2409-5710.2025.12.2>

ABSTRACT

This study presents a comparative evaluation of ensemble generation techniques for projecting wind speed in the state of Rio Grande do Norte, Brazil, utilizing regional climate models from the CORDEX initiative. Two approaches—Arithmetic Mean (AM) and Convex Combination (CC)—were assessed for the historical period (1994–2023) and for future projections (2031–2060) under the high-emission RCP 8.5 scenario. The findings demonstrate that the AM method consistently outperforms CC, exhibiting higher correlation coefficients and lower root mean square error (RMSE) values across all subregions analyzed. Specifically, the AM ensemble achieved correlation coefficients of 0.88, 0.86, and 0.80 in the northern, central, and eastern regions, respectively, exceeding those of the CC method (0.85, 0.84, and 0.78). Relative to present-day conditions, projected future wind speeds increase by approximately 12.2% in the northern region, 23.5% in the eastern region, and 19.6% in the central region. A notable seasonal shift was also observed, with peak wind speeds occurring later in the year across all areas. These projected increases, when considered in light of the cubic relationship between wind speed and energy production, suggest that wind power potential may rise by over 40% in certain regions. It is also important to acknowledge that such results are subject to uncertainties inherent in climate modeling, including the structural differences among regional and global models and their associated physical parameterizations. Nonetheless, the projected enhancement in wind speed holds significant implications for strategic renewable energy planning in Rio Grande do Norte and reinforces the utility of multi-model ensemble techniques in climate-based energy assessments.

*Corresponding Author
Email: augusto.rubim@ifrn.edu.br

1. Introduction

Climate change and its associated impacts have become central topics of global scientific and political discourse in recent years. A key driver of increased greenhouse gas (GHG) emissions is electricity generation from non-renewable sources. In response, expanding power production from renewable energy has emerged as one of the most effective strategies to reduce emissions and mitigate the effects of climate change [1]. In Brazil, there has been notable growth in electricity generation from wind and solar sources.

Unlike most countries, Brazil already derives the majority of its electricity from renewable sources. As of 2024, approximately 85% of the country's 200 gigawatts (GW) of installed electrical capacity comes from clean energy. However, the Brazilian energy matrix remains heavily dependent on hydroelectric power, which accounted for 50.3% of total electricity generation in 2023, according to the Brazilian Wind Energy Association [2]. This reliance on hydropower is concerning, particularly in light of Brazil's recurring droughts, such as those experienced in the Northeast Region (NEB) between 2012 and 2017 [3].

Wind energy has become the second-largest source of electricity in Brazil, contributing 15.9% of the national total in 2023 [2]. That year, Brazil had 1,027 operational wind farms, with a combined installed capacity of 30.45 GW—an 18.79% increase over 2022, when the capacity stood at 25.63 GW [2]. The favorable conditions in 2023 positioned Brazil as the third-largest installer of wind farms globally, behind only the United States and China.

Within Brazil, the Northeast Region plays a leading role in wind energy production, accounting for 92% of the country's wind-generated electricity. Between 2022 and 2023, the region experienced a 19% increase in wind energy output, while the North Region saw a comparatively modest growth of 8% [2].

The Northeast's strong wind energy performance is primarily attributed to its unique geographical and atmospheric conditions. The region is influenced by the Intertropical Convergence Zone (ITCZ) and trade winds, both of which provide steady and directionally consistent airflow throughout the year [4]. It is also affected by the South Atlantic Subtropical Anticyclone (SASA), which intensifies during the second half of the year, further enhancing wind speeds [5].

Assessing wind energy potential is crucial for strategic planning and investment decisions. A thorough understanding of regional wind patterns is essential for evaluating the viability of wind farm development. While such assessments are typically based on data from meteorological stations, these datasets are often incomplete, inconsistent, or temporally sparse, reducing their reliability. Moreover, standard measurements are taken at 10 meters above ground, whereas modern wind turbines operate at heights closer to 100 meters. This discrepancy necessitates the use of supplementary methods to accurately estimate wind energy potential [6].

To overcome these limitations, researchers increasingly rely on reanalysis datasets. A leading source of such data is the European Centre for Medium-Range Weather Forecasts (ECMWF), which provides the ERA5 reanalysis. This dataset spans from 1950 to the present and offers a horizontal resolution of $0.25^\circ \times 0.25^\circ$ [7]. For projecting future climate conditions, climate models are widely employed. In South America, the Regional Climate Model (RCM) RegCM4.7—developed under the framework of the Coordinated Regional Climate Downscaling Experiment (CORDEX-CORE)—is commonly used [8]. Its proven ability to simulate temperature and precipitation fields [9, 10] makes it a dependable tool for regional climate analysis.

One of the key approaches recommended by the IPCC for projecting future wind speed involves the use of Representative Concentration Pathways (RCPs). This study adopts the RCP 8.5 scenario, which represents a high-emission pathway in which radiative forcing is projected to reach 8.5 W/m^2 by the year 2100 as a result of increasing greenhouse gas (GHG) concentrations [9, 10].

The RCP 8.5 scenario was selected because it reflects a trajectory characterized by minimal mitigation efforts and continued high emissions. This allows for the assessment of the most substantial potential changes in climate, offering insights into extreme impacts under a business-as-usual development model. Although RCP 8.5 is currently considered less likely due to the adoption of more ambitious climate policies, it remains a critical

benchmark in climate impact studies. It is particularly relevant for identifying risks and informing long-term adaptation strategies. For example, [11] employed RCP 8.5 to evaluate future offshore wind energy resources, highlighting its importance in guiding infrastructure investment and policymaking under worst-case scenarios. Similarly, [12] used this pathway to assess the sensitivity of European wind power potential to climate change, reinforcing the utility of high-emission scenarios for exploring upper-bound variability in renewable energy resources. RCP 8.5 also serves as a reference for numerous global and regional modeling experiments, having been designed as the upper boundary scenario in the original RCP framework [13].

Projections of climate variables, particularly wind speed, are inherently subject to several sources of uncertainty. These include internal climate variability, differences in the structure and parameterization of climate models, and the uncertainty associated with future emission trajectories. Recent studies have identified internal variability as one of the leading contributors to uncertainty in wind energy projections, alongside inter-model spread and scenario dependency [14]. In addition, systematic biases in climate models—such as the misrepresentation of physical processes or the limitations imposed by coarse spatial resolution—can significantly affect the fidelity of wind projections [15]. Identifying, quantifying, and accounting for these sources of uncertainty is essential to support robust, evidence-based decision-making in the energy sector and to facilitate the design of effective adaptation strategies.

Despite the importance of such assessments, studies that focus explicitly on future wind speed projections remain limited and often rely on simplified approaches. For instance, [9, 10] employed ensemble techniques based on the arithmetic mean of climate model outputs. Meanwhile, [16] restricted their analysis to individual models under present-day climate conditions. A more advanced strategy was proposed by [17], who introduced alternative ensemble generation methods—such as Convex Combination and Principal Component Regression—which were shown to outperform the arithmetic mean, especially in future projection contexts. Building on this evidence, the present study incorporates the Convex Combination (CC) approach as a robust ensemble generation methodology.

As demonstrated by [18] ensemble techniques that apply convex combination weighting schemes have shown superior performance in short-term wind speed forecasting, yielding more stable and accurate prediction intervals. In the context of this study, Convex Combination is employed to improve the skill of wind speed projections by assigning weights to individual model outputs based on their past performance. [17] demonstrated that the CC approach outperformed the arithmetic mean when applied to future climate simulations, particularly for variables with high spatial and temporal variability, such as wind speed. This methodology enhances the precision of climate signal extraction and reduces the impact of poorly performing models, thereby increasing the reliability of projections for wind resource assessment and energy planning.

The primary contribution of this research lies in addressing the scarcity of high-resolution wind speed projections for future scenarios, with a particular focus on wind power potential. This study concentrates on the state of Rio Grande do Norte, Brazil's leading wind energy producer, and conducts an in-depth analysis of three distinct sub-regions. In addition to adopting a novel ensemble strategy, the aim is to reduce projection uncertainty for both wind speed and wind power density, thereby enhancing the utility of the results for long-term infrastructure and policy planning.

The three selected areas within Rio Grande do Norte were chosen based on two core criteria. First, each area exhibits a high density of operational wind farms, making them relevant case studies for current and future wind energy exploration. Second, they are situated in climatically diverse zones of the state, allowing for a broader and more comparative assessment of regional atmospheric dynamics [17]. A detailed description of the climatological characteristics and model validation for each area is provided in the Materials and Methods section.

From a planning perspective, it is important to emphasize that the areas identified as having the highest average wind speeds in this study correspond to those with the greatest concentration of installed wind infrastructure, as previously reported by [16]. This spatial alignment between modeled wind potential and existing development underscores the practical relevance of the projections, particularly for expanding and optimizing renewable energy strategies at both local and regional levels.

The overarching goal of this research is to compare ensemble methods based on regional climate models from the CORDEX initiative, applied to the state of Rio Grande do Norte during the historical period (1994–2023), and to project future wind speed for the mid-century period (2031–2060) under the RCP 8.5 scenario. The method that exhibits the best performance will be adopted to generate wind speed forecasts with reduced uncertainty, thereby supporting more accurate wind energy planning.

2. Materials and Methods

2.1. Study Area

We examined three areas in this study: 1) Eastern Rio Grande do Norte, 2) Northern Rio Grande do Norte, and 3) Central Rio Grande do Norte. Fig. (1) shows the location of these areas.

The selection of the three study areas in Rio Grande do Norte was based on their high density of installed wind farms, as reported by [16]. Additionally, the areas were chosen to represent distinct geographical and climatic characteristics, allowing for a more comprehensive analysis of wind patterns across diverse sub-regions.



Source: Adapted from: www.baixarmapas.com.br

Figure 1: Location of Rio Grande do Norte on the map of the Northeast region and the study areas.

The eastern region of Rio Grande do Norte, encompassing the state capital Natal, is characterized by a tropical Atlantic climate with high humidity and precipitation concentrated between May and August, influenced by easterly wave systems. Wind speeds in this area remain relatively stable throughout the year, ranging from 2.9 to 5.2 m/s, with an average between 4.3 and 4.4 m/s, as determined by Weibull distribution analysis. This consistency is largely due to the prevailing southeast trade winds originating from the Atlantic Ocean [19]. The Mato Grande region (including João Câmara) stands out for its high density of wind farms, accounting for approximately 56% of Rio Grande do Norte's installed wind energy capacity. The region benefits from strong winds throughout most of the year, a result of its strategic geographic location where trade winds curve around the South American

continent [19]. The northern region, including areas such as the Chapada do Apodi, exhibits a semi-arid climate with average annual temperatures around 28.5°C and an average annual precipitation of 772 mm. Winds in this area average 7.5 m/s, with higher intensities observed during the second half of the year, enhancing its suitability for wind energy generation.

2.2. Data

2.2.1. ECMWF-ERA5 Reanalysis

The ERA5 reanalysis dataset, developed by the European Centre for Medium-Range Weather Forecasts (ECMWF), is distributed through the Copernicus Climate Data Store and represents the fifth generation of reanalysis products [7]. In this study, we utilized monthly mean wind speed data at 100 meters above ground level for the period 1994–2023 to represent present-day conditions. The dataset features a uniform horizontal resolution of $0.25^\circ \times 0.25^\circ$ in both latitude and longitude. ERA5 was used as the observational reference in this study, serving as a substitute for in situ meteorological station data [7].

2.2.2. Regional Climate Models

For future projections, we employed the Regional Climate Model (RCM) RegCM4.7 [20], developed as part of the CORDEX-CORE initiative [8]. This RCM was driven by three distinct Global Climate Models (GCMs): HadGEM2-ES [21], NorESM1-M [22], and MPI-ESM-MR [23]. Each GCM provides boundary conditions based on its own physical and mathematical framework, resulting in variations in the downscaled climate simulations [24].

Wind speed outputs from RegCM4.7 were obtained on a monthly timescale for the period 1994–2060, with an original spatial resolution of $0.22^\circ \times 0.22^\circ$. To ensure consistency in model validation, these outputs were bilinearly resampled to match the $0.25^\circ \times 0.25^\circ$ resolution of the ERA5 dataset.

While RCMs are widely used for downscaling global climate projections and refining spatial detail, their outputs are subject to inherent uncertainties that may affect the accuracy of wind speed simulations. A primary source of uncertainty stems from the large-scale boundary conditions imposed by the driving GCMs. These conditions can introduce systematic biases, which are then inherited by the regional models. As noted by [25], the performance of RCMs is closely tied to the quality of their GCM inputs—an issue commonly referred to as the "garbage in, garbage out" principle. Moreover, [26] emphasized that physical parameterizations in climate models are typically based on empirical constants derived from specific climatic regions, potentially introducing additional biases when applied to different geographic contexts such as the Northeastern region of Brazil (NEB).

2.3. Methodology

2.3.1. Model Ensembles

Multi-model ensembles are widely adopted in climate science to reduce uncertainties in future projections. By integrating outputs from multiple individual models, ensemble techniques enhance forecast reliability through the combination of their unique characteristics. This integration helps smooth inter-model discrepancies and mitigate systematic errors, ultimately improving model performance and confidence in projections [27–30].

The first known application of an arithmetic mean ensemble to simulate meteorological variables in South America was conducted by [31], yielding promising results. Building upon this foundation, the present study evaluates and compares two ensemble generation methodologies: the Arithmetic Mean (AM) and the Convex Combination (CC).

2.3.1.1. Arithmetic Mean (AM)

The arithmetic mean is one of the most widely used statistical measures, representing the central tendency of a set of values. In the context of climate modeling, it involves calculating the simple average of outputs from multiple models. The arithmetic mean at a given time t is defined as, equation (1):

$$AM_t = \frac{1}{n} \sum_{i=1}^n V_{i,t} \quad (1)$$

Where: AM_t is the arithmetic mean at time t for the n models, n is the total number of models, $V_{i,t}$ is the wind speed in model i at time t , t represents time.

2.3.1.2. Convex Combination (CC)

The convex combination is an advanced ensemble method that assigns weights to each model based on its performance relative to reference observations [17]. A key property of this method is that all weights are strictly positive and sum to 1, ensuring a balanced and interpretable contribution from each model.

In this study, model weights are determined using the Mean Squared Error (MSE). Originally proposed by [17, 32] for precipitation simulations over South America, the use of MSE was shown to enhance model skill. Given its robustness in capturing discrepancies between model output and observations, this metric was also applied here to wind speed simulations.

The MSE is defined as [33]:

$$EQM = \frac{1}{n} \sum_{i=1}^n [mod_i - obs_i]^2 \quad (2)$$

The weighted mean, based on MSE, is given by Equation (3):

$$\bar{x}_l = \frac{(\sum_{i=1}^n \frac{1}{EQM_{Mi}} x M_i)}{\sum_{i=1}^n \frac{1}{EQM_{Mi}}} \quad (3)$$

where: mod_i is the value of the Regional Climate Models, and obs_i is the value of the reanalysis; N is the number of observations, M_i is the model forecast, with $i=1,2,...,8$

2.3.2. Monthly Variability of Wind Speed at 100m Above Ground in RN Areas

To evaluate the monthly variability of wind speeds during the present-day period (1994–2023), a descriptive statistical analysis was conducted for each study area in the state of Rio Grande do Norte. Wind speed data at 100 meters above ground level were examined using **boxplots**, which allow for the visualization of seasonal trends, interquartile ranges, and potential outliers. This analysis provides a clearer understanding of wind behavior across different months and regions.

2.3.3. Comparison Between Methodologies and Models – Taylor Diagram

According to [24], one of the most comprehensive and visually intuitive methods for assessing model performance is the Taylor Diagram [34]. This graphical tool enables the simultaneous evaluation of three essential statistical metrics: Root Mean Square Error (RMSE) [36], Pearson Correlation Coefficient [36], Standard Deviation [34]. These three metrics are standard outputs of the `taylor` function available in the R programming environment, which is commonly used in climate data analysis. The choice of these metrics follows established practices in the literature and ensures consistency with statistical tools broadly adopted in the climate modeling community.

In the Taylor Diagram, the reanalysis data are plotted along the x-axis as the reference point. Model outputs and ensemble estimates are displayed as points in a Cartesian space, where proximity to the reference point indicates higher agreement with observed data.

Table 1 summarizes the equations used to compute each of these statistical indicators (Equations 4–6).

Where: P_{ens} corresponds to the ensemble data; P_{obs} corresponds to the observed data; n representing the number of observations. $P_{obs,i}$ is the observed value at time i ; \bar{P}_{obs} is the mean observed value; $P_{ens,i}$ is the

estimated value in the ensemble at time i ; \bar{P}_{ens} is the mean estimated value of the ensemble; r is the Pearson correlation coefficient. $\sigma_{obs(mod)}$ is the Standard Deviation of the observations and ensemble.

The equation (6) is used to calculate de standard deviation of the observations and after from ensemble data.

Table 1: Summary of the equations used in the Taylor Diagram.

Key metrics	Equation
Root Mean Square Error	$RMSE = \sqrt{\frac{1}{N} \sum_{i=1}^n (p_{ens} - P_{obs})^2}$ (4)
Pearson Correlation Coefficient	$r = \frac{\sum_{i=1}^n (P_{obs,i} - \bar{P}_{obs})(P_{ens,i} - \bar{P}_{ens})}{\sqrt{\sum_{i=1}^n (P_{obs,i} - \bar{P}_{obs})^2 \times (\sum_{i=1}^n (P_{ens,i} - \bar{P}_{ens})^2)}}$ (5)
Standard Deviation	$\sigma_{obs(mod)} = \sqrt{\frac{(P_{obs,i} - \bar{P}_{obs})^2}{(n-1)}}$ (6)

2.3.4. Comparison of Wind Speed at 100m Above Ground Using the Best Methodology for Present and Future

At this stage of the study, a climatological analysis of the data will be conducted by calculating the monthly climatological mean for the entire analyzed period. Through line graphs, it will be possible to assess wind speed trends over time, identifying potential increases or decreases in wind intensity for the future (2031-2060), based on the best ensemble methodology identified for the present period (1994-2023).

3. Results and Discussion

3.1. Monthly Variability of Wind Speed at 100m Above Ground in RN Areas

Fig. (2-4) illustrate wind variability in the northern, eastern, and central (João Câmara region) parts of Rio Grande do Norte from 1994 to 2023, respectively.

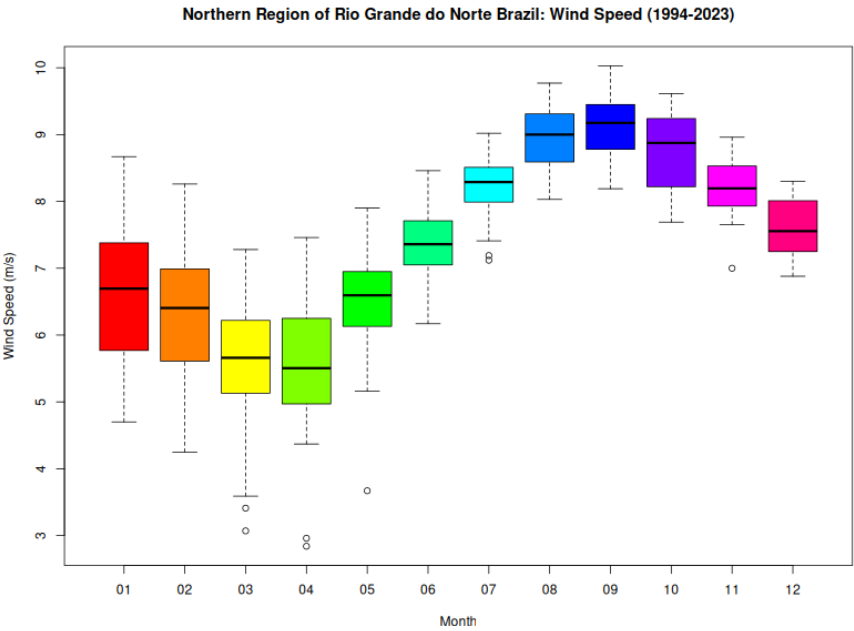


Figure 2: Wind variability in the northern part of Rio Grande do Norte for the present (1994-2023).

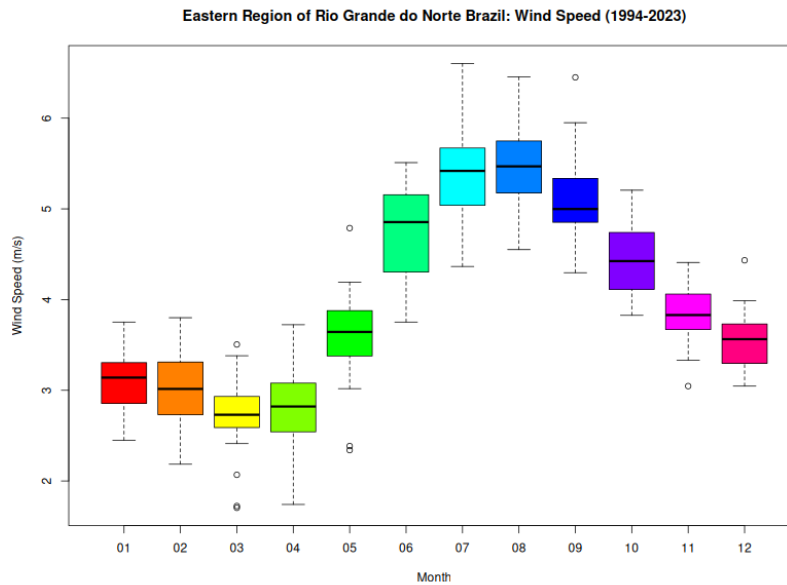


Figure 3: Wind variability in the eastern part of Rio Grande do Norte for the present (1994-2023).

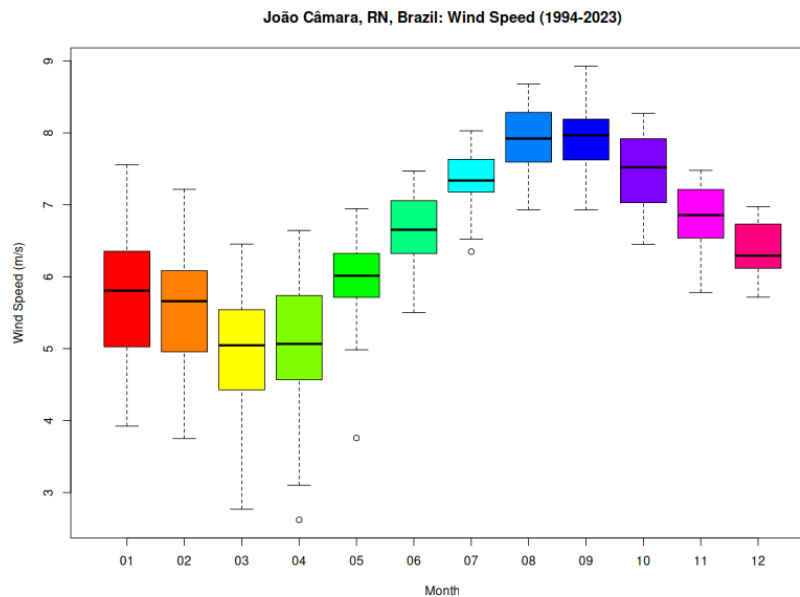


Figure 4: Wind variability in the central part of Rio Grande do Norte for the present (1994-2023).

The climatological analysis of wind speed at 100 m above ground level in Rio Grande do Norte (1994-2023) reveals distinct seasonal patterns. The analysis of the boxplot graphs reveals a clear seasonal variability in average wind speeds across the three studied regions of Rio Grande do Norte (RN), Brazil: the northern, central (João Câmara), and eastern areas. It is evident that the highest mean wind speeds occur between August and November, whereas the lowest values are recorded between March and May.

Specifically, in the eastern region, average wind speeds range from approximately 2.5 m/s in March to 6.5 m/s in September. In the central region, wind speeds vary between 3.5 m/s in April and 8.5 m/s in September. The northern region exhibits the highest values, with averages ranging from 4.0 m/s in March to 9.5 m/s in September. These patterns indicate a marked intensification of wind activity in the second half of the year, particularly between August and November.

The seasonal variability observed in wind speeds is closely linked to the dynamics of large-scale atmospheric systems, notably the South Atlantic Subtropical Anticyclone (SASA). During the austral winter, SASA tends to shift

toward lower latitudes, intensifying wind flow over northeastern Brazil. This southward displacement enhances the atmospheric pressure gradient, thereby increasing wind speeds across the region [5, 7].

In addition to the influence of SASA, the Intertropical Convergence Zone (ITCZ) plays a crucial role in modulating the seasonal distribution of wind in the region. During August and September, the ITCZ migrates northward in response to shifts in the thermal equator. This migration amplifies thermal gradients between the continent and the adjacent Atlantic Ocean, reinforcing the southeast trade winds and mesoscale circulations such as sea breezes—particularly along coastal and adjacent inland areas [37]. According to [38], the ITCZ, formed by the convergence of northeasterly and southeasterly trade winds, is a key component of tropical atmospheric circulation. Its seasonal movement not only shapes rainfall patterns but also directly affects wind regimes across northern South America, including northeastern Brazil.

Climatic phenomena such as El Niño and La Niña also play an important role in the interannual variability of wind speeds. During El Niño events, higher wind speeds are generally observed, whereas La Niña years tend to be associated with reduced wind intensities. These variations reflect the broader influence of the El Niño–Southern Oscillation (ENSO) on regional atmospheric dynamics [39].

Previous studies further corroborate the findings of this research. For example, [16] identified that the northern regions of Rio Grande do Norte and Ceará exhibit the highest wind power densities, particularly between August and November. Likewise, [39] observed that wind speeds in central Northeast Brazil tend to peak between July and November and reach their minimum between March and April.

Understanding these spatiotemporal patterns is critical for optimizing the planning and operation of wind power generation in the region. Identifying the months with the most favorable wind conditions enables better resource allocation and enhances the operational efficiency of wind farms, particularly in semi-arid and coastal zones where seasonal variation is pronounced.

3.2. Comparison Between Methodologies and Models – Taylor Diagram

Fig. (5-7) present Taylor diagrams for the recent past, illustrating model performance in the northern, eastern, and central (João Câmara) regions of Rio Grande do Norte, respectively.

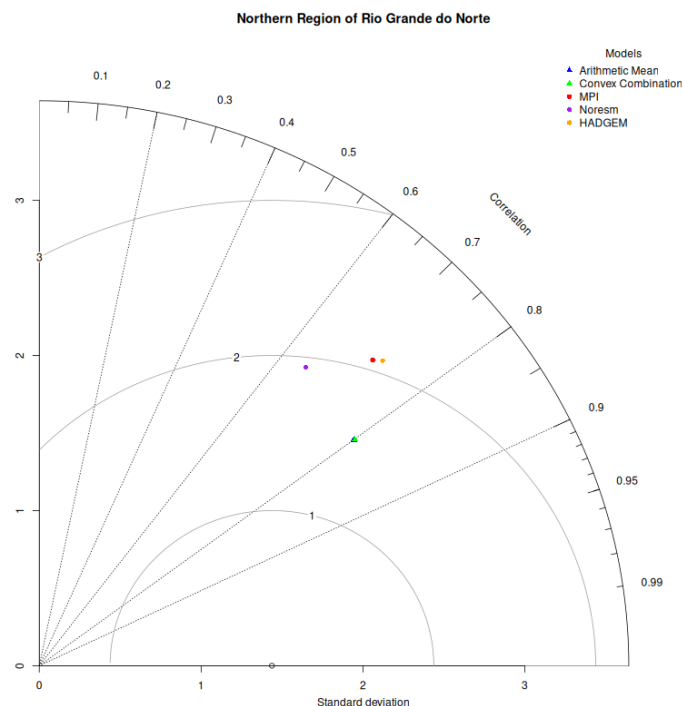


Figure 5: Taylor diagram for the northern area of Rio Grande do Norte for the present.

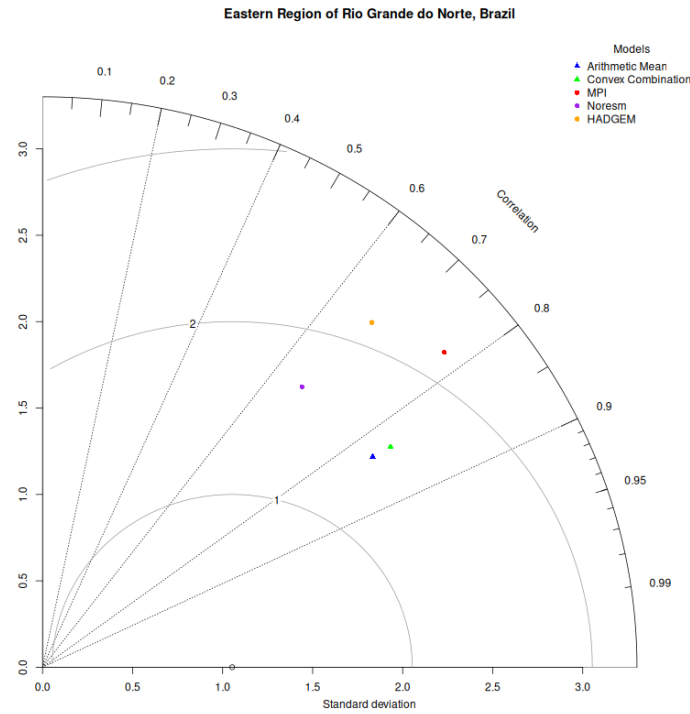


Figure 6: Taylor diagram for the eastern area of Rio Grande do Norte for the present.

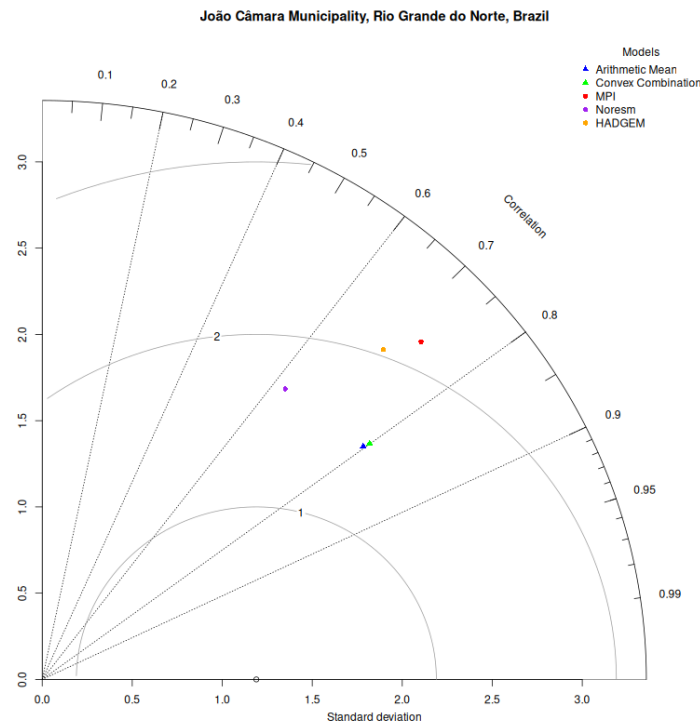


Figure 7: Taylor diagram for the central area of Rio Grande do Norte for the present.

The Taylor diagrams indicate that the Arithmetic Mean (AM) generally outperforms the Convex Combination (CC) across all study regions. In the northern region of Rio Grande do Norte, AM achieved a correlation coefficient of 0.88 and a root mean square error (RMSE) of 1.0 m/s, compared to CC's correlation of 0.85 and RMSE of 1.2 m/s. In the eastern region, AM recorded a correlation of 0.80 and RMSE of 1.4 m/s, also surpassing CC, which had a correlation of 0.78 and RMSE of 1.6 m/s. Similarly, in the central region (João Câmara), AM performed slightly better (correlation = 0.86; RMSE = 1.0 m/s) than CC (correlation = 0.84; RMSE = 1.1 m/s).

This outcome contrasts with the findings of [17], who argued that the convex combination method is statistically superior due to its ability to minimize ensemble error through the weighted contribution of each model. The discrepancy may stem from regional differences in model error distributions. While CC is theoretically more effective in scenarios with divergent model biases, AM may perform better when models exhibit comparable error structures. These findings support the recommendation by [31], who emphasize that the effectiveness of ensemble methods must be evaluated locally, according to the behavior of the individual models and the target variable.

Furthermore, three individual models—MPI, NorESM, and HADGEM—demonstrated lower performance across all domains, with reduced correlation and increased RMSE. This supports the consensus in the literature that ensemble approaches consistently outperform individual models, offering more robust and less volatile approximations of observed [27, 40].

The discrepancies in model performance can be further explained by underlying uncertainties in model structure and boundary conditions. Firstly, regional models are sensitive to their driving global models (GCMs), which may propagate systematic biases related to the representation of synoptic-scale features such as pressure gradients and jet streams [41]. Secondly, scenario assumptions—particularly regarding greenhouse gas concentrations and aerosol forcing—affect how the models simulate future climate conditions. In this study, all projections were based on the RCP 8.5 scenario, which assumes high emissions and minimal mitigation.

Additional uncertainties stem from the physical parameterizations of atmospheric processes—especially those governing boundary-layer turbulence, convection, and surface roughness—which directly influence the simulation of wind speed. The spatial resolution also plays a critical role: coarse-resolution models are less able to resolve mesoscale processes such as sea breezes and topographic flows, which are essential for accurate wind energy assessments in coastal environments like Rio Grande do Norte. These uncertainties were also addressed by [17], who emphasized the importance of selecting the ensemble technique and individual members that exhibit the best statistical performance in each specific area to reduce uncertainty in wind resource estimation.

Therefore, although the arithmetic mean method demonstrated superior statistical metrics in this analysis, the overarching conclusion remains: ensemble methods—regardless of their specific formulation—offer a more reliable basis for regional wind projections than any single model. This insight is essential for guiding future assessments of wind energy potential in the Brazilian Northeast, where minimizing uncertainty is critical for sustainable energy planning.

3.3. Comparison of Wind Speed at 100m Above Ground Using the Best Methodology for Present and Future

Fig. (8-10) present the wind speed climatologies for the northern, eastern, and central regions of Rio Grande do Norte, respectively. These climatologies were developed using the best statistical method identified in section 3.2: the arithmetic mean. The figures compare the projected future wind speed climatology (2025–2054) with the past climatology (1994–2023) using the same technique. Additionally, the comparisons include the ERA5 reanalysis dataset, which serves as a reference.

The statistical analysis of wind speed climatologies for these three regions reveals significant future trends, including increases in wind intensity and changes in seasonality, as projected by the ensemble based on the AM.

In the northern region, the maximum wind speed in the past (ERA5) was 9.8 m/s in September. Future projections indicate an increase to 11.0 m/s, with the peak month shifting to October. Meanwhile, the minimum wind speed, which was 5.5 m/s in April, slightly decreases to 5.2 m/s and shifts to May. These changes suggest a prolongation of the strong wind season, possibly linked to alterations in regional atmospheric circulation.

In the eastern region, the projected increase in wind speed is even more pronounced. The maximum speed, previously 7.5 m/s in September, rises to 10.2 m/s in October, signaling a substantial enhancement in the region's wind power potential. The minimum speed also increases, from 3.5 m/s in March to 4.8 m/s in April. The shift in maximum and minimum wind speeds may be linked to modifications in trade wind dynamics and the strengthening of the SASA, which influences regional wind patterns.

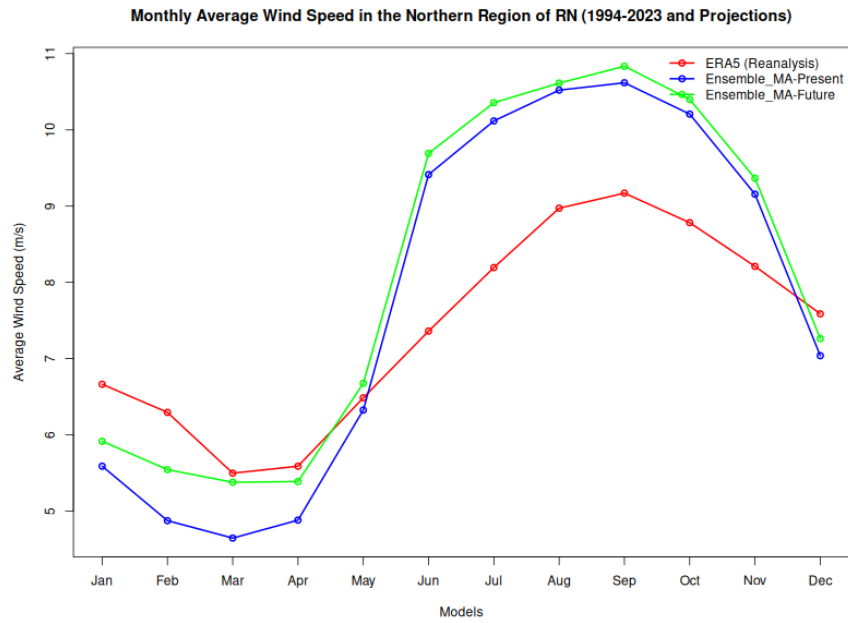


Figure 8: Comparison of wind speed climatology between the past and the future for the northern region of Rio Grande do Norte.

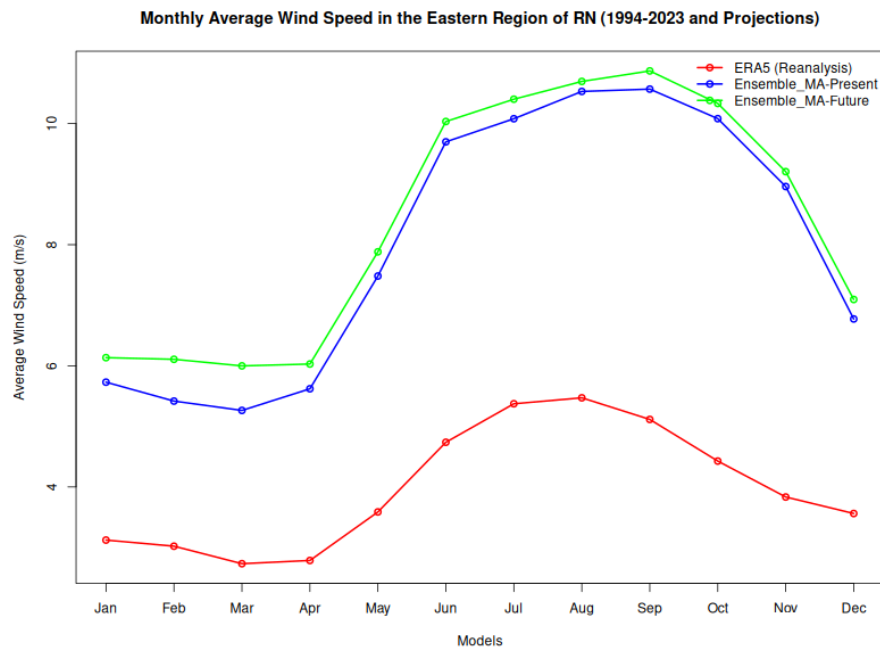


Figure 9: Comparison of wind speed climatology between the past and the future for the eastern region of Rio Grande do Norte.

In the central region, the maximum wind speed, which occurred in August at 8.5 m/s, is now projected for September at 10.5 m/s. The minimum wind speed increases from 4.8 m/s in March to 5.3 m/s in April. This region, already known for its high wind power density, could benefit even further from this projected intensification.

These results align with previous studies that project a future increase in wind speeds due to atmospheric circulation changes [9]. However, the observed shifts in seasonal wind patterns—particularly the delay in peak speeds—warrant further investigation. One possible explanation is the delayed intensification of the South Atlantic Subtropical Anticyclone (SASA), as suggested in studies of wind variability in South America [5].

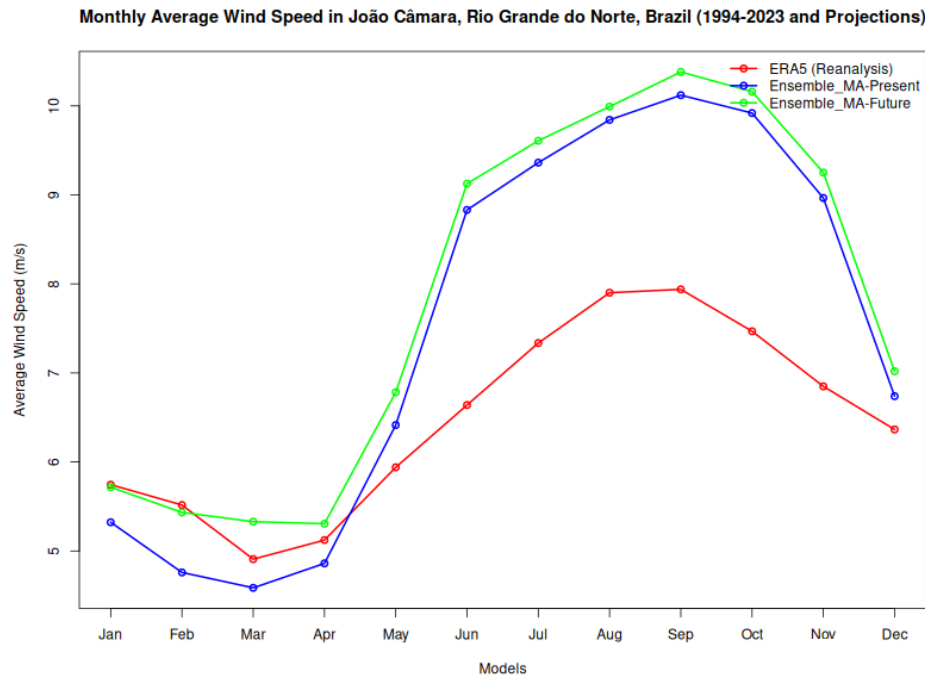


Figure 10: Comparison of wind speed climatology between the past and the future for the central region of Rio Grande do Norte.

The increase in wind speed directly implies growth in wind energy potential. According to the wind power equation, energy generation is proportional to the cube of wind speed, meaning that a 10% increase in wind speed could result in approximately a 33% increase in wind power generation [16].

These findings are crucial for energy planning in Rio Grande do Norte, Brazil's leading wind energy producer, as they highlight the potential for expanding wind farm capacity and optimizing infrastructure to accommodate evolving wind patterns.

These projections underscore the critical role of climate modeling in accurately assessing future wind power potential and guiding strategic energy investments in the region.

4. Conclusion

The results of this study indicate that the ensemble technique based on the Arithmetic Mean (AM) performed better than the Convex Combination (CC), contradicting previous studies that suggested greater effectiveness of CC. This suggests that, for the studied region, model weighting may not provide significant advantages when individual models exhibit similar error patterns. However, this outcome may not be directly generalizable to other regions with different climatic dynamics or error structures across models, and future studies should evaluate the robustness of these findings under varying geographic and climatic conditions. Additionally, the results reinforce the reliability of using ensembles over individual models, reducing uncertainties in climate projections. Nonetheless, potential sources of uncertainty remain, including model resolution limitations, boundary condition assumptions, and internal variability that may influence the ensemble performance.

The projected increase in wind speed and the shift in peak intensity months may be related to the intensification of the South Atlantic Subtropical Anticyclone (SASA) and changes in atmospheric circulation patterns. Since wind power is proportional to the cube of wind speed, the results suggest a significant increase in wind energy generation in the future. While this trend appears promising, it is important to consider whether the observed intensification could also lead to increased variability or more frequent extreme wind events, which may pose operational challenges for wind energy infrastructure. Moreover, it remains to be investigated whether

similar patterns would emerge in other subtropical regions, which could have important implications for global renewable energy planning.

These findings highlight the importance of climate modeling in developing strategies for the expansion of renewable energy in Brazil. They also provide valuable insights for regional energy policy and infrastructure planning, supporting the optimization of wind farm siting and long-term investment strategies. A limitation of this study is the focus on a single RCP scenario and a specific subset of regional models; exploring alternative emissions trajectories and incorporating additional model outputs could offer a more comprehensive assessment.

Future research should consider testing additional RCP scenarios and further refining ensemble techniques using a broader range of regional climate models, as well as investigating how these changes in wind regimes interact with local socioeconomic and environmental factors.

Conflict of Interest

The authors declare that there is no conflict of interest.

Funding

We thank IFRN for the financial support provided to the scholarship holder Roberta Doca, whose contribution was fundamental to the development of this article.

Availability of Data and Material

ECMWF-ERA5

<https://cds.climate.copernicus.eu/datasets?q=era5&kw=Variable+domain%3A+Atmosphere+%28surface%29&kw=Variable+domain%3A+Atmosphere+%28upper+air%29&kw=Variable+domain%3A+Atmosphere+%28upper+level%29&kw=Variable+domain%3A+Ocean+%28physics%29>

CORDEX-CORE

<https://esgf-ui.ceda.ac.uk/cog/search/esgf-ceda/>

References

- [1] Hamed TA, Alshare A. Environmental impact of solar and wind energy- a review. *J Sustain Dev Energy Water Environ Syst.* 2022; 10(2): 1090387. <https://doi.org/10.13044/j.sdewes.d9.0387>
- [2] Associação Brasileira de Energia Eólica – ABEEólica. ABEEólica. Available at: <https://abeeolica.org.br/> (accessed on September 3, 2024).
- [3] Marengo JA, Torres RR, Alves LM. Drought in Northeast Brazil—Past, present, and future. *Theor Appl Climatol.* 2017; 129(3-4): 1189-200. <https://doi.org/10.1007/s00704-016-1840-8>
- [4] Vásquez P IL, Barbosa HA, Sampaio G, Sánchez P CA, Utida G, Quispe DP, *et al.* Multidecadal variability of the ITCZ from the Last Millennium Extreme Precipitation Changes in Northeastern Brazil. *EGUsphere.* 2022; 2022: 1-26. <https://doi.org/10.5194/egusphere-2022-785>
- [5] Reboita MS, Ambrizzi T, Silva BA, Pinheiro RF and da Rocha RP. The South Atlantic Subtropical Anticyclone: Present and future climate. *Front Earth Sci.* 2019; 7: 8. <https://doi.org/10.3389/feart.2019.00008>
- [6] Ruiz SAG, Barriga JEC, Martínez JA. Wind power assessment in the Caribbean region of Colombia, using ten-minute wind observations and ERA5 data. *Renew Energy.* 2021; 172: 158-76. <https://doi.org/10.1016/j.renene.2021.03.033>
- [7] Hersbach H, Bell B, Berrisford P, Hirahara S, Horányi A, Muñoz-Sabater J, *et al.* The ERA5 global reanalysis. *Q J R Meteorol Soc.* 2020; 146(730): 1999-2049. <https://doi.org/10.1002/qj.3803>
- [8] Giorgi F, Jones C, Asrar G. Addressing climate information needs at the regional level: the CORDEX framework. *WMO Bull.* 2009;58(3):175. Available from: <https://www.adaptation-changement-climatique.gouv.fr/sites/cracc/files/inline-files/CORDEX1.pdf> (accessed on Jan 13, 2025).
- [9] Reboita MS, Amaro TR, de Souza MR. Winds: Intensity and power density simulated by RegCM4 over South America in present and future climate. *Clim Dyn.* 2018; 51: 187-205. <https://doi.org/10.1007/s00382-017-3913-5>

- [10] Sawadogo W, Reboita MS, Faye A, Rocha RP, Odoulami RC, Olusegun CF, *et al.* Current and future potential of solar and wind energy over Africa using the RegCM4 CORDEX-CORE ensemble. *Clim Dyn.* 2021; 57: 1647-72. <https://doi.org/10.1007/s00382-020-05377-1>
- [11] Gross M, Magar V. Offshore wind energy climate projection using UPSCALE climate data under the RCP8.5 emission scenario. *PLoS One.* 2016; 11(10): e0165423. <https://doi.org/10.1371/journal.pone.0165423>
- [12] Davy R, Gnatiuk N, Pettersson L, Bobylev L, Climate change impacts on wind energy potential in the European domain with a focus on the Black Sea, *Renew Sustain Energy Rev.* 2018; 81(2): 1652-9. <https://doi.org/10.1016/j.rser.2017.05.253>
- [13] Riahi K, Rao S, Krey V, Cho C, Chirkov V, Fischer G, *et al.* RCP 8.5—A scenario of comparatively high greenhouse gas emissions. *Clim Change.* 2011; 109: 33-57. <https://doi.org/10.1007/s10584-011-0149-y>
- [14] Wu R, Niu X, Jing X, Li P, Mao Y, Chen X, *et al.* Future projection and uncertainty analysis of wind and solar energy in China based on an ensemble of CORDEX-EA-II regional climate simulations. *J Geophys Res Atmos.* 2024; 129(6): e2023JD040271. <https://doi.org/10.1029/2023JD040271>
- [15] Wu Y, Miao C, Fan X, Miao C. Quantifying the uncertainty sources of future climate projections and narrowing uncertainties with bias correction techniques. *J Adv Model Earth Syst.* 2022; 14(11): e2022MS003392. <https://doi.org/10.1029/2022EF002963>
- [16] Gurgel ARC, Sales DC, Lima KC. Wind power density in areas of Northeastern Brazil from regional climate models for a recent past. *PLoS One.* 2024; 19(7): e0307641. <https://doi.org/10.1371/journal.pone.0307641>
- [17] Coutinho MDL, Lima KC, Santos e Silva CM. Improvements in precipitation simulation over South America for past and future climates via multi-model combination. *Clim Dyn.* 2017; 49: 343-61. <https://doi.org/10.1007/s00382-016-3346-6>
- [18] Long H, Geng R, Zhang C. Wind speed interval prediction based on the hybrid ensemble model with biased convex cost function. *Front Energy Res.* 2022; 10: 954274. <https://doi.org/10.3389/fenrg.2022.954274>
- [19] Barros JD, Furtado MLS, Costa AMB, Marinho GS, Silva FM. Sazonalidade do vento na cidade de Natal/RN pela distribuição de Weibull. *Soc Territ.* 2013; 25(2): 78-92.
- [20] Elguindi N, Giorgi F, Solmon F, Gao X, Rauscher S, Coppola E, *et al.* Regional climate model RegCM: Reference manual version 4.7. Trieste: Abdus Salam ICTP; 2017. Available from: https://www.researchgate.net/profile/Muhammadreza_Tabatabaei/post/Uncertainty_in_Climate_Models/attachment/59eef385b53d2fe117b8794c/AS:552896195502080%401508832133118/download/ReferenceMan.pdf
- [21] Collins WJ, Bellouin N, Doutriaux-Boucher M, Gedney N, Halloran P, Hinton T, *et al.* Development and evaluation of an Earth-system model – HadGEM2. *Geosci Model Dev.* 2011; 4: 1051-1075. <https://doi.org/10.5194/gmd-4-1051-2011>
- [22] Zhang ZS, Nisancioglu K, Bentsen M, Tjiputra J, Bethke I, Yan Q, *et al.* Pre-industrial and mid-Pliocene simulations with NorESM-L. *Geosci Model Dev.* 2012; 5(2): 523-33. <https://doi.org/10.5194/gmd-5-523-2012>
- [23] Zanchettin D, Rubino A, Matei D, Bothe O, Jungclaus JH. Multidecadal-to-centennial SST variability in the MPI-ESM simulation ensemble for the last millennium. *Clim Dyn.* 2012; 40(6): 1301-18. <https://doi.org/10.1007/s00382-012-1361-9>
- [24] Ambrizzi T, Reboita MS, Rocha RP, Llopart M. The state of the art and fundamental aspects of regional climate modeling in South America. *Ann N Y Acad Sci.* 2019; 1436(1): 98-120. <https://doi.org/10.1111/nyas.13932>
- [25] Giorgi F, Mearns LO. Approaches to the simulation of regional climate change: A review. *Rev Geophys.* 1991; 29(2): 191-216. <https://doi.org/10.1029/90RG02636>
- [26] Takle ES, Roads J, Rockel B, Gutowski WJ, Arritt RW, Meinke I, *et al.* Transferability intercomparison: An opportunity for new insight on the global water cycle and energy budget. *Bull Am Meteorol Soc.* 2007; 88(3): 375-84. <https://doi.org/10.1175/BAMS-88-3-375>
- [27] Tebaldi C, Knutti R. The use of the multi-model ensemble in probabilistic climate projections. *Philos Trans A Math Phys Eng Sci.* 2007; 365(1857): 2053-75. <https://doi.org/10.1098/rsta.2007.2076>
- [28] Yazd HRGH, Salehnia N, Kolsoumi S, Hoogenboom G. Prediction of climate variables by comparing the k-nearest neighbor method and MIROC5 outputs in an arid environment. *Clim Res.* 2018; 76(4): 303-18. <https://doi.org/10.3354/cr01545>
- [29] Hagedorn R, Doblas-Reyes FJ, Palmer TN. The rationale behind the success of multi-model ensembles in seasonal forecasting – I. Basic concept. *Tellus A Dyn Meteorol Oceanogr.* 2005; 57(3): 219-33. <https://doi.org/10.3402/tellusa.v57i3.14657>
- [30] Knutti R, Abramowitz G, Collins M, Eyring V, Gleckler PJ, *et al.* Good practice guidance paper on assessing and combining multi model climate projections. In: Stocker TF, Qin D, Plattner G-K, Tignor M, Midgley PM, Eds. Meeting Report of the IPCC Expert Meeting on Assessing and Combining Multi Model Climate Projections. Bern, Switzerland: IPCC Working Group I Technical Support Unit, University of Bern; 2010. p. 1-15.
- [31] Coutinho MM. Previsão por Conjunto Utilizando Perturbações Baseadas em Componentes Principais. Master's Dissertation, National Institute for Space Research (INPE), São José dos Campos, Brazil 1999.
- [32] Paiva AP, Ferreira JR, Paiva EJ, Balestrassi PP, Costa SC. A multivariate mean square error optimization of AISI 52100 hardened steel turning. *Int J Adv Manuf Technol.* 2008; 43: 631-43. <https://doi.org/10.1007/s00170-008-1745-5>
- [33] Andrade DDF. Métodos Quantitativos – Pesquisa Operacional. Vol. III. Belo Horizonte: Poisson; 2018.
- [34] Taylor KE. Summarizing multiple aspects of model performance in a single diagram. *J Geophys Res.* 2001; 106(D7): 7183-92. <https://doi.org/10.1029/2000JD900719>
- [35] Wilks DS. Statistical Methods in the Atmospheric Sciences. 3rd ed. Oxford: Academic Press; 2011.
- [36] Devore JL. Probability and Statistics for Engineering and the Sciences. São Paulo: Thomson Pioneira; 2006. p. 706.

- [37] Reboita MS, Krusche N, Ambrizzi T, Rocha RP. Entendendo o tempo e o clima na América do Sul. *Terra Didat*. 2012; 8(1): 34-50. Available from: <https://www.ige.unicamp.br/terraedidatica/v8-1/pdf81/s3.pdf>
- [38] Ribeiro RMR, Vitorino MI, Moura MN. Variabilidade sazonal da Zona de Convergência Intertropical e sua influência sobre o norte da América do Sul. *Rev Bras Geogr Fis*. 2023; 16(5): 2798-810. <https://doi.org/10.26848/rbgf.v16.5.p2798-2810>
- [39] Santos ATS, Silva CMS. Seasonality, interannual variability, and linear tendency of wind speeds in the Northeast Brazil from 1986 to 2011. *Sci World J*. 2013; 2013: Article ID 490857. <https://doi.org/10.1155/2013/490857>
- [40] Weigel AP, Knutti R, Liniger MA, Appenzeller C. Risks of model weighting in multimodel climate projections. *J Clim*. 2010; 23(15): 4175-91. <https://doi.org/10.1175/2010JCLI3594.1>
- [41] Brands S, Herrera S, Fernández J, Gutiérrez JM. How well do CMIP5 Earth System Models simulate present climate conditions in Europe and Africa? *Clim Dyn*. 2013; 41(3): 803-17. <https://doi.org/10.1007/s00382-013-1742-8>